Gold Bull (2017) 50:319–326
https://doi.org/10.1007/s13404-017-0222-z

ORIGINAL PAPER

Au/CuMgAl-hydrotalcite catalysts promoted by Cu^+ and basic sites for selective oxidation of glycerol to dihydroxyacetone

Yanrui Yin[1,2] · **Tian Tang**[1,2] · **Chunli Xu**[1,2]

Received: 28 June 2017 / Accepted: 2 November 2017 / Published online: 22 November 2017

Abstract CuMgAl-hydrotalcite-supported Au catalysts were prepared and tested in the selective conversion of glycerol to dihydroxyacetone. The electron density of Au was decreased by Cu embedded in the supports, arising from the electron transfer from Au to Cu sites. The valence state (+ 1) of Cu ions was detected. Both Cu^+ and basic sites (Mg–O) affected the catalytic activity of Au catalysts. The Cu^+ sites promoted the selective oxidation of glycerol to dihydroxyacetone, while basic sites boosted the selectivity oxidation of glycerol to glyceric acid. The synergy of Cu^+ sites and basic sites could effectively promote the activity and selectivity of Au catalysts in the selectively conversion of glycerol to dihydroxyacetone. A 53% conversion of glycerol and 72% of dihydroxyacetone selectivity were obtained under optimum reaction conditions.

Keywords Glycerol oxidation · Au catalyst · Cu^+ sites · Basic sites · Dihydroxyacetone

Introduction

Much attention has been given to transformation of glycerol (GL) to value-added fine chemicals and fuel [1, 2], especially through the routes of oxidation. GL is a highly functionalized molecule and contains two primary OH groups and one secondary OH group [3]. Oxidation of GL is a very complex process, including multiple parallel reactions, and generating a variety of products, such as glyceraldehyde (GLD), dihydroxyacetone (DHA), glyceric acid (GLA), tartronic acid (TAA), oxalic acid (OXA), glycolic acid (GLCA), glyoxylic acid (GA), and formic acid (FA) [4, 5]. Therefore, controlling the reaction selectivity is necessary to obtain the desired products. DHA, formed by oxidation of the secondary OH groups of GL, is one of the desirable products. It is an economically interesting product, applying in cosmetics industry as a self-tanning agent and the fine chemicals industry as a chemical intermediate in organic synthesis [6, 7]. Controlling the selectivity to DHA depends on the design of catalysts [8].

Au catalysts had attracted considerable attention as promising aerobic alcohol oxidation catalysts owing to the high selectivity and resistance against over-oxidation [9]. Liu et al. [10] reported the performance of Au NPs on different oxides in catalyzing GL oxidation for DHA formation at elevated temperature. Especially, Au/CuO catalyst exhibited a high DHA selectivity. However, the catalytic activity of Au/CuO catalyst was low for the transformation of GL to DHA.

The activity of Au could be promoted by base, such as NaOH or basic supports [10–12]. However, the main product was GLA, not DHA, when using Au as catalysts in the presence of base promoters [13]. Since the activity of Au could be promoted by basic sites and the selectivity to DHA could be adjusted by Cu sites [10], we prepared Au/CuMgAl-HTs catalysts, which contained metal sites (Au), basic sites (Mg–O), and Cu^+ sites. The synergy of basic sites and Cu^+ sites on the activity of Au catalysts and the selectivity to DHA for GL oxidation was investigated for the aim to increase both the activity and selectivity of Au catalysts in the transformation of GL to DHA.

Electronic supplementary material The online version of this article (https://doi.org/10.1007/s13404-017-0222-z) contains supplementary material, which is available to authorized users.

✉ Chunli Xu
xuchunli@snnu.edu.cn

[1] Key Laboratory of Applied Surface and Colloid Chemistry, Ministry of Education, Shaanxi Normal University, Xi'an 710119, People's Republic of China

[2] School of Chemistry and Chemical Engineering, Shaanxi Normal University, Xi'an, People's Republic of China

Experimental

Preparation of supports

A series of supports were prepared by a co-precipitation method as described in our report [14]. Typically, a total concentration of 1.5 M mixed aqueous solution of $Cu(NO_3)_2{\cdot}3H_2O$, $Mg(NO_3)_2{\cdot}6H_2O$, and $(Al(NO_3)_3{\cdot}9H_2O)$ were dissolved in 160 mL of deionized water by continuous stirring with an alkaline solution of Na_2CO_3−NaOH. The pH of the mixture was kept at values between 9.5 and 10.5. The molar ratio of CO_3^{2-} to Al^{3+} was 2:1. After being aged at 60 °C for 18 h with stirring, the slurry was filtered and washed. The precipitate was dried at 110 °C for 12 h. The obtained materials were denoted as CuMgAl-HTs (Cu/Mg/Al, 1:1:1, 1:4:1, 1:5:1, 1:7:1, 1:9:1, 1:13:1, 1:15:1, 1:20:1, 1:30:1).

The MgAl-HTs (9:1) supports were prepared by the similar procedure as CuMgAl-HTs, with the pH of slurry keeping at 10 without the $Cu(NO_3)_2{\cdot}3H_2O$ aqueous solution. CuAl-HTs sample was prepared by using a similar procedure without the $Mg(NO_3)_2{\cdot}6H_2O$ aqueous solution.

Synthesis of the Ausupported catalyst

The Au/CuMgAl-HTs catalysts were prepared by an impregnation−reduction approach [15]. Typically, the CuMgAl-HTs supports were added to $HAuCl_4{\cdot}4H_2O$ (1 mg/mL) aqueous solution under vigorous stirring. After 1 h of vigorous stirring at room temperature, the slurry was stirred at 85 °C for 1.5 h, followed by drying at 100 °C for 12 h, and reduction in H_2 at 300 °C for 2 h. If there is no other special statement, the amount of theoretical Au loading is 1 wt%.

The Au/MgAl-HTs (9:1), Au/CuO, and Au/CuAl-HTs catalysts were prepared according to the above steps. The Au loadings was 1 wt%.

Catalyst characterization

The Micromeritics ASAP 2020 instrument was used to measure the surface area, pore characteristics, and average pore diameter of the materials. The samples were degassed at 140 °C for 4 h. Nitrogen adsorption/desorption isotherms were calculated at 77 K, the relative pressure range from 0.06 to 0.30. Total pore volumes were estimated at a relative pressure of 0.995.

X-ray diffraction (XRD) patterns were estimated over a D/Max-2550VB+PC x-ray powder diffractometer (Rigaku Co., Japan), using a Cu–Ka source fitted with an Inel CPS 120 hemispherical detector. The scanning transmission electron microscopy (STEM), and energy-dispersive x-ray were conducted on a Tecnai G2F20 (USA).

CO_2-temperature-programmed desorption (CO_2-TPD) were performed on a Micromeritics AutoChem 2920 II instrument. The position and area of the desorption peak are directly correlated with the basic strength and basic amount, respectively. Typically, the sample was pretreated with high-purity He at 350 °C for 1 h. After cooling to 50 °C, CO_2 adsorption was performed by switching the He flow to 10% CO_2/He gas mixture at 100 °C for 1 h. The gas−phase (and/or weakly adsorbed) CO_2, was purged by high-purity He at the same temperature. CO_2-TPD was then performed in the He flow by raising to 800 °C at a rate of 10 °C min^{-1}. The desorbed CO_2 were detected by MKS Cirrus 2 mass spectrometer.

X-ray photoelectron spectra (XPS) were conducted on an AXIS ULTRA spectrometer (Kratos Analytical Ltd., Japan) with Al Kα x-ray source (1486.6 eV, 15 kV, 5 mA) at energy of 150 W. In this study, XPS was used to measure the valence of Au and Cu. Chemical analyses of metals were performed by using inductively coupled plasma mass spectrometry (ICP-MS, M90, Bruker).

Reaction procedure

GL oxidation was carried out in 100-ml polytetrafluoroethylene-lined stainless steel autoclaves (Parr autoclaves). The catalyst of 0.088 g and GL solution (0.3 M) were admitted into the reactor, purged with oxygen, and adjusted to the desired pressure of 3 bar, heated to 60 °C for 4 h, cooled to room temperature. Using high-pressure liquid chromatography (HPLC) equipped with refractive index and ultraviolet detectors to analyze the reaction mixture. Authentic samples were used to identify products. An external calibration method was used to quantify the products and reactants remained.

Results and discussion

Catalyst characterization

BET surface area and pore size analysis

The nitrogen physisorption data of supports and Au catalysts are shown in Table 1. Increasing the Mg content resulted in continued lowering of the surface area of CuMgAl-HTs supports from 93 to 3 $m^2\ g^{-1}$. The pore volume of the supports also decreased from 0.66 to 0.018 $cm^3\ g^{-1}$ (entries 1–5). The specific surface areas of supports increased after Au doping. For example, the surface area of Au/CuMgAl-HTs (1:30:1) was up to 174 $m^2\ g^{-1}$, which was attributed to the high temperature reduction process resulting in the formation of mixed oxides [15]. The catalysts' pore volume also decreased from 0.85 to 0.32 $cm^3\ g^{-1}$ with the increase of Mg content. The nitrogen adsorption isotherms of the samples exhibited the characteristic type IV shape [16], together with the pore size

Table 1 Nitrogen physisorption data of CuMgAl-HTs supports and Au catalysts with different Cu/Mg/Al molar ratio

Entry	Cu/Mg/Al	Supports/catalysts		
		BET surface area ($m^2\ g^{-1}$)[a]	Pore diameter (Å)[b]	Pore volume ($cm^3\ g^{-1}$)[b]
1	1:1:1	93/111	285/306	0.66/0.85
2	1:4:1	39/140	259/133	0.25/0.47
3	1:9:1	35/166	202/99	0.18/0.41
4	1:20:1	27/142	228/95	0.16/0.34
5	1:30:1	3/174	330/74	0.018/0.32

[a] Calculated by the BET method

[b] Calculated by the BJH method from the desorption isotherm

distribution results, suggested that the samples were mesoporous materials (Figs. S1 and S2).

The crystalline phases of samples

The XRD patterns of Au/CuMgAl-HTs catalysts with different Cu/Mg/Al molar ratio were shown in Fig. 1. These results showed the diffraction peaks of MgO, which were observed irrespective of the Cu/Mg/Al molar ratio and distinct from the corresponding peaks of their supports (Fig. S3). Moreover, the Cu_2O diffraction peaks were observed. Increasing the content of Mg, that is, lowering the content of Cu, the diffraction peak intensity of Cu_2O was weaker. The results showed that the basic sites (Mg–O) coexisted with metal sites Cu^+ in our catalysts. No diffraction peaks corresponding to Au were observed for catalysts, which may be attributed to its low loading or low size [17].

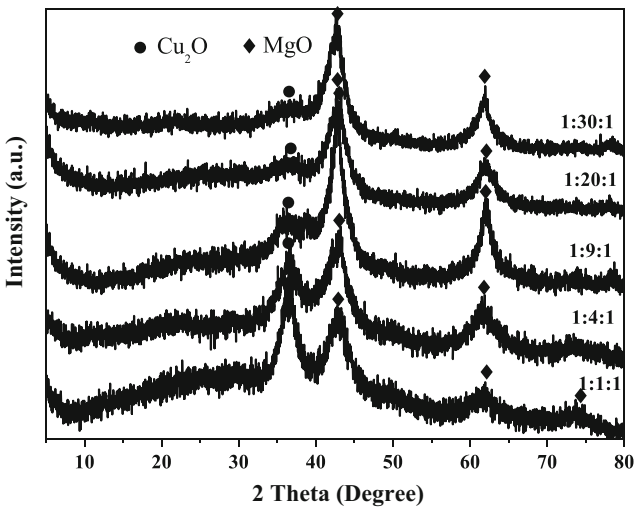

Fig. 1 XRD patterns of Au/CuMgAl-HTs samples with different Cu/Mg/Al molar ratio

The size and composition of catalysts

The morphology and structural of Au/CuMgAl-HTs samples were characterized by STEM. As shown in Fig. 2, the size of Au NPs gradually decreased with increasing Mg content. The average size was approximately 5.0 nm with Cu/Mg/Al molar ratio of 1:1:1. The size of Au NPs was 3.2 nm for molar ratio of 1:4:1. Lower mean size of 2.0–2.5 nm was observed for Au NPs with molar ratio of 1:9:1 (or 1:20:1, 1:30:1). The difference in size of Au NPs can be attributed to the content and the dispersion of Cu in the supports, which played an important role in the dispersion of the Au NPs. In our former reports, it was found that the dispersion of Cu ions, as configurational ion of HT supports, could control the dispersion of the Au NPs through their interaction [15].

The base properties of catalysts

The basicity of the Au/CuMgAl-HTs catalysts was determined by the CO_2-TPD. As shown in Fig. 3, the desorption peaks located at similar position for all the samples, which contained two desorption peaks at 100 and 425 °C, respectively. It suggested that the Au/CuMgAl-HTs catalysts contained weak basic sites and medium basic sites. The desorption peaks differed in height and width. Increasing the content of Mg resulted in the increase in the height and width of the desorption peaks, such as the desorption peaks height of Au/CuMgAl-HTs with Cu/Mg/Al molar ratio of 1:30:1 was twice of that for Cu/Mg/Al molar ratio of 1:1:1 at 100 °C. This indicated that the Cu/Mg/Al molar ratio markedly affects the base properties of Au catalysts.

XPS analysis

As shown in Fig. 4a, the XPS spectra of Au/CuMgAl-HTs showed peaks of the Au $4f_{5/2}$ and Au $4f_{7/2}$ states. Increasing the content of Cu resulted in the positive shifts to higher BE of Au $4f_{7/2}$, moving from 83.8 to 84.5 eV, which may be attributed to the transfer of electrons from Au to Cu.

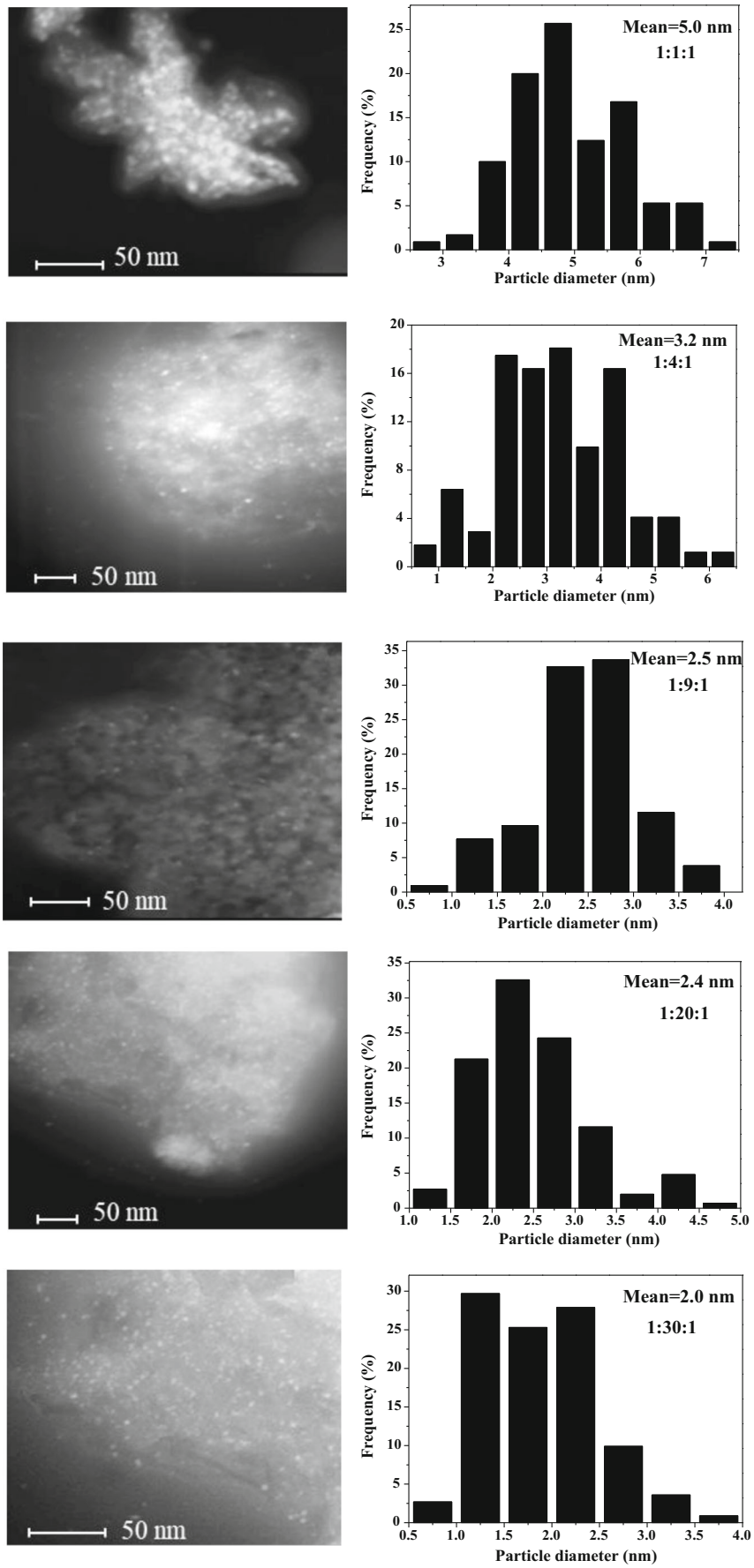

Fig. 2 STEM images and particle size distributions for Au/CuMgAl-HTs with different Cu/Mg/Al molar ratio

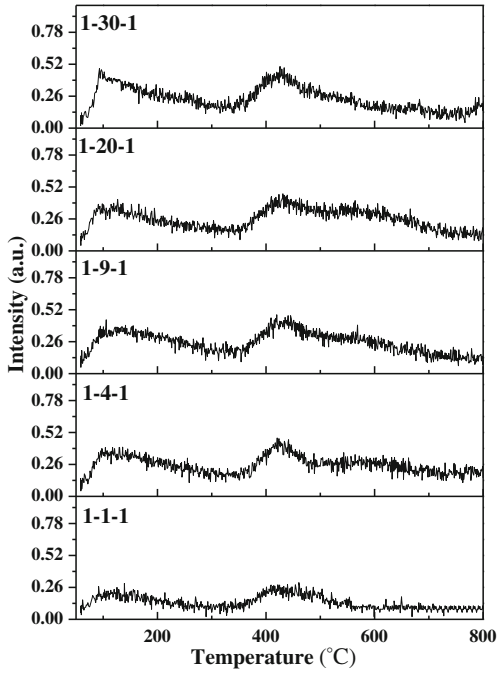

Fig. 3 CO_2-TPD profiles of Au/CuMgAl-HTs catalysts with different Cu/Mg/Al molar ratio

Figure 4b showed the XPS spectra of the Cu 2p region. The BE of Cu $2p_{3/2}$ was 932.5 eV and no satellite peaks was observed, suggesting that the catalysts may not contain Cu^{2+} because the BE of Cu^{2+} was 933.6 eV and accompanied by the characteristic Cu^{2+} satellite peaks (938–945 eV). Therefore, it was presumed the presence of Cu^{+} or Cu^{0} species in catalyst. It is quite difficult to distinguish the chemical states of Cu^{+} or Cu^{0} species, because of the similar electron binding energy and peak shape [18]. Auger Cu LMM spectra [19] can be used to distinguish the Cu^{+} and Cu^{0} species. The kinetic energy (KE) of Cu was at ~ 916.3 eV (Fig. 4c), which corresponds to the Cu^{+}. In combination with the spectrum of Cu $2p_{3/2}$ and Cu LMM, it can deduce that Cu^{2+} was reduced to Cu^{+} in the process of preparing the catalyst of Au/MgCu-HTs. The measured results were in agreement with XRD data. However, they were different from the results by Xu et al. [10], in which the valence state of Cu was 2+.

The effect of basic sites and Cu^{+} sites on GL oxidation

As shown in Table 2, the catalytic performance of the supports and Au catalysts for GL oxidation was investigated. The GL

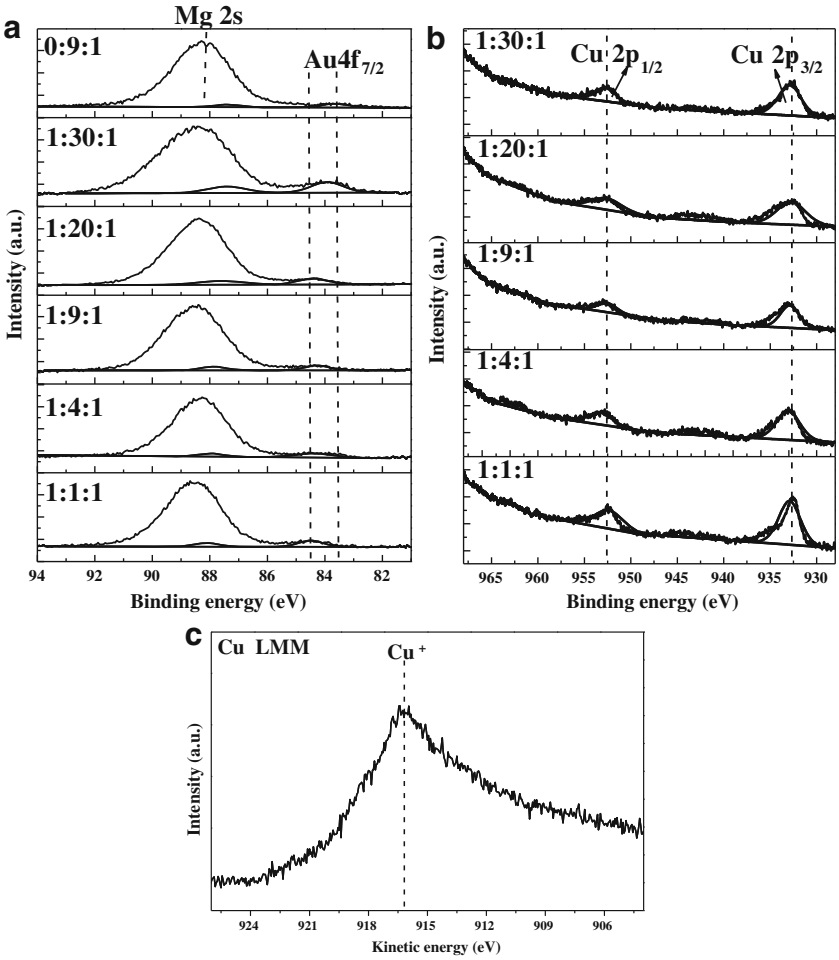

Fig. 4 XPS spectra of Au/CuMgAl-HTs catalysts with different Cu/Mg/Al molar ratios. **a** Au 4f XP spectra. **b** Cu 2p XP spectra. **c** XAES spectra of Cu LMM for Au/CuMgAl-HTs (1:1:1) catalysts

Table 2 Activity and selectivity for GL oxidation over different supports and catalysts

Entry	Catalysts	TOF (h^{-1})[b]	GL conv. (%)	Product selectivity (%)						
				GLA	GLCA	TAA	GA	OXA	DHA	FA
1	CuAl-HTs	–	< 1	–	–	–	–	–	–	–
2	MgAl-HTs	–	1.7	42.9	11.4	–	–	3.9	–	33
3	CuMgAl-HTs	–	3.8	50.0	13.0	–	–	5.1	–	28
4	Au/CuAl-HTs	5	4.5	–	–	–	–	5.2	92.0	–
5	Au/MgAl-HTs	19	18.0	45.0	6.0	8.0	2.6	6.8	28.0	–
6	Au/CuMgAl-HTs	292	42.0	11.0	8.6	2.2	–	10.0	64.0	4

[a] Reaction conditions: 15 mL, 0.3 M GL, 1 wt% Au, GL/Au = 1000 mol/mol, 60 °C, P_{O2} = 3 bar, stirring speed = 400 rpm, time = 4 h, Mg/Al = 9:1, Cu/Mg/Al = 1:9:1

[b] Turn over frequency = (mole of glycerol converted after 0.5 h)/(reaction time (0.5 h) × mole of total loading of gold); the amount of catalyst was 0.088 g

conversion of the pure supports (CuAl-HTs, MgAl-HTs, CuMgAl-HTs) as catalysts were low. The maximum GL conversion was 3.8% for CuMgAl-HTs (entry 3). MgAl-HTs exhibited the next activity, which was 1.7% (entry 2). The CuAl-HTs showed the lowest activity (GL conversion, < 1%). The basic sites (Mg–O) and metal ions (Cu) sites were coexisted in CuMgAl-HTs. The MgAl-HTs contained only basic sites (Mg–O). While for CuAl-HTs supports, it had only metal ions (Cu) sites. It indicated that the basic sites facilitated the activity of supports. The results also showed that the basic sites of Mg–O and metal ions (Cu) sites together promoted the activity of CuMgAl-HTs for GL oxidation.

The catalytic activity increased after Au doping. The maximum of GL conversion was 42% (Entry 6) for Au/CuMgAl-HTs. It indicated that the Au sites acted as the active sites for GL oxidation. Moreover, Au/CuMgAl-HTs was the most active catalyst, next was Au/MgAl-HTs, and Au/CuAl-HTs showed the lowest activity. The results were further demonstrated by TOF. The TOF value was 292 h^{-1} for Au/CuMgAl-HTs (entry 6), 19 h^{-1} for Au/MgAl-HTs (entry 5), and 5 h^{-1} for Au/CuAl-HTs (entry 4). The difference in the activity of three Au catalysts indicated that catalytic activity of Au was affected by their supports. Either basic sites or metal ions (Cu^+) in supports could promote the catalytic activity of Au catalysts for GL oxidation. However, the coexistence of basic sites and metal ions (Cu^+) in supports was better than single sites in promoting the activity of Au.

The products distribution over pure supports and Au catalysts for GL oxidation was shown in Table 2. When the pure supports (MgAl-HTs, CuMgAl-HTs) were used as catalysts, the main products were GLA and FA. The selectivity toward GLA was in the range of 40–50%. The selectivity to FA was around 30%. This indicated that the pure supports promoted the formation of over-oxidation products. While the products mainly included DHA and GLA after Au doping. The Au/CuAl-HTs catalyst exhibited the highest DHA selectivity of 92% (entry 4). The next highest selectivity to DHA was 64% for Au/CuMgAl-HTs (entry 6). The lowest selectivity to DHA of 28% was observed for Au/MgAl-HTs (entry 5). The results demonstrated that Cu^+ sites promoted the selectivity to DHA for GL oxidation by Au catalysts. For the selectivity to GLA, Au/MgAl-HTs catalyst exhibited the highest selectivity of 45% (entry 5). Next was Au/CuMgAl-HTs with 11% of the selectivity to GLA. However, no GLA was found for Au/CuAl-HTs catalyst. The oxidation of the primary OH groups of GL sequentially generates GLA. It indicated that the basic sites could promote the oxidation of primary OH groups of GL.

XPS analysis showed that there was electron transfer from Au sites to Cu^+ sites. It was also reported that Cu sites were active in dehydrogenation of secondary alcohol [20, 21], where the valence of Cu was 0 or + 2. However, no reports showed the activity of Cu^+ sites in dehydrogenation of secondary alcohol. Therefore, it was not sure whether the effect of Cu^+ sites on activity and selectivity of Au sites was from the decrease in electron density of Au sites or the direct activation of Cu^+ sites on secondary alcohol. Further study will be conducted in our future work.

Effect of Cu/Mg/Al molar ratio on GL oxidation over Au catalysts

The basic sites and Cu^+ sites of supports not only affect the GL conversion, but also the products selectivity over Au catalysts. In order to increase both the activity and selectivity of Au catalysts, the effect of the amounts of the basic sites and Cu^+ sites on GL oxidation was investigated by changing Cu/Mg/Al molar ratio.

The activity of Au/CuMgAl-HTs versus Cu/Mg/Al molar ratio for GL oxidation were shown in Table 3. When the Cu/Mg/Al molar ratio was 1:1:1, the GL conversion was low, only 8% (entry 1). Increasing the Mg content (or decreasing the Cu content) resulted in increasing the GL conversion. The maximum GL conversion was 46% (entry 7), as the Cu/Mg/Al molar ratio was 1:15:1. Then, the GL conversion decreased to 16% with

Table 3 Effect of Cu/Mg/Al molar ratio on activity and selectivity of Au/CuMgAl-HTs for GL oxidation

Entry	Cu/Mg/Al	GL conv. (%)	Product selectivity (%)					
			GLA	GLCA	TAA	OXA	DHA	FA
1	1:1:1	8	9.2	7.3	–	9.6	47.0	6.8
2	1:4:1	23	12.0	7.5	2.1	12.0	62.5	0.6
3	1:5:1	26	12.0	8.5	2.1	11.0	66.0	0.6
4	1:7:1	33	9.9	8.1	2.3	10.4	66.0	3.2
5	1:9:1	42	11.0	8.6	2.2	10.0	64.0	4.0
6	1:13:1	43	12.0	12.3	3.2	11.2	52.4	8.0
7	1:15:1	46	10.1	12.9	1.9	10.2	50.0	10.0
8	1:20:1	21	33.0	16.1	3.9	13.2	19.1	7.0
9	1:30:1	16	33.0	18.6	4.6	12.9	16.5	5.0

[a] Reaction conditions: 1 wt% Au/CuMgAl-HTs, others see the footnote of Table 2

the Cu/Mg/Al molar ratio of 1:30:1 (entry 9). It demonstrated that the Cu/Mg/Al molar ratio affected the activity of the Au/CuMgAl-HTs catalysts. The specific surface area of Au/CuMgAl-HTs with different Cu/Mg/Al molar ratios (Table 1) did not have direct relation with their activity. Au/CuMgAl-HTs (1:30:1) performed low GL conversion but the maximum specific surface area. As mentioned before, Au/CuMgAl-HTs catalysts contained Au, basic, and Cu^+ sites. Modulating of the molar ratio of Cu/Mg/Al resulted in the change of the amounts of the basic sites and Cu^+ sites. Thus, the amounts of the basic sites and Cu^+ sites affected the GL conversion.

The selectivity to DHA was 47% when Cu/Mg/Al molar ratio was 1:1:1. It reached to 62–66% when Cu/Mg/Al molar ratio was in the range of 1:4:1~1:9:1 (entries 2–5). The selectivity to DHA began to decrease with increasing the Mg content (or decreasing the Cu content; entries 6–9). It decreased to 16.5%, as the Cu/Mg/Al molar ratio was 1:30:1 (entry 9). It indicated that the appropriate amounts of basic sites and Cu^+ sites promoted the selective oxidation of glycerol to DHA over Au catalysts. The selectivity to GLA changed slightly in the range of 9.2–12.0% (entries 1–7) when content of Mg was low. When the Mg content was high, i.e., Cu/Mg/Al molar ratio was 1:20:1 or 1:30:1, the selectivity to GLA increased to 33% (entry 8). The results showed that the amounts of basic sites affect the selectivity to GLA. It was found that the similar phenomena were observed for the selectivity to GLCA (or TAA, OXA). Thus, it indicated that the basic sites promoted the oxidation of primary OH group and the over-oxidation of products. The possible reaction pathway was shown in Scheme 1.

The size of Au nanoparticles normally affected its catalytic performance [22]. The size for Au/CuMgAl-HTs with 1:9:1 of Cu/Mg/Al molar ratio was similar with that of 1:20:1 of Cu/Mg/Al molar ratio (Fig. 2). The similar size eliminated the effect of size on activity of Au. However, they showed different catalytic performance. The former generated 42% of GL conversion (Table 2, entry 5), while the latter got 21% of GL conversion. This further demonstrated that the difference in Au catalysts was resulted from the effect of Cu sites and basic sites, but not the size of Au nanoparticles.

The effect of reaction conditions and the stability of catalysts

The effect of reaction conditions, such as reaction time, temperature, and catalyst dosage was investigated (Table S1). Under optimum reaction conditions, 0.088 g of 1 wt% Au/CuMgAl-HTs catalyst at a temperature of 60 °C, and Cu/Mg/Al molar ratio of 1:9:1, the conversion of GL reached 53%, and the selectivity to DHA was up to 72%.

The post-reaction solutions were tested for metal (Au, Cu, Mg, and Al) by inductively coupled plasma mass spectrometry (ICP-MS) and the leaching rates of metals were showed in Table S2. Leaching rate of all the metals was less than 15%. The reaction was conducted for 2 h and then the catalyst was filtered out to observe whether the reaction continued after the catalyst was removed (4 h). The conversion of glycerol over 2 h was 27% and remained unchanged over 4 h after the catalyst removed. This could prove that there was no apparent homogeneous catalysis taking place in the glycerol oxidation for Au/CuMgAl-HTs.

Fig. S4a–c shows XRD patterns of Au/MgAl-HTs, Au/CuAl-HTs, and Au/CuMgAl-HTs catalysts before and after reaction. The XRD pattern of Au/MgAl-HTs before and after reaction were similar, displaying typical diffraction peak of HTs at 11.33°, 22.84°, 34.74°, and 39.13° and MgO at 43.1°

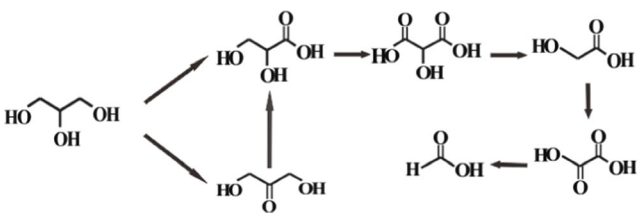

Scheme 1 Reaction pathway for GL oxidation

and 62.3° before reaction. The XRD patterns of Au/CuAl-HTs before and after reaction were also similar, showing diffraction patterns characteristic of Cu, CuO, and Cu_2O with a difference in the intensity of Cu. Au/CuAl-HTs after reaction displayed weaker diffraction peak of Cu. Au/CuMgAl-HTs before reaction showed diffraction peak of MgO and Cu_2O. The pattern of Au/CuMgAl-HTs after reaction displayed characteristic peak of HTs, CuO, and MgO. This indicated that Cu_2O was oxidized to CuO in the reaction system and the support partly transformed back to structure of HTs.

The reusability of Au/CuMgAl-HTs was investigated and showed in Table S3 (supporting information).The conversion of glycerol on fresh catalyst was 53%. The conversion decreased to 47, 43, and 39% in the first, second, and third run. During the recycle, the descent rate of glycerol conversion was approximately 10%. Thus, the deactivation of the catalysts was not significant and further proved a better stability and reused activity of the used catalyst.

Conclusions

The synergy of Cu^+ sites and basic sites (Mg–O) promoted the activity of Au catalyst. GL conversion was 42% for Au/CuMgAl-HTs containing both Cu^+ sites and basic sites, which was far higher than that of Au/MgAl-HTs containing only basic sites (18%) and Au/CuAl-HTs containing only Cu^+ sites (4.5%). The Cu^+ sites in Au/CuMgAl-HTs and Au/CuAl-HTs activated the second OH groups of GL to selectively generate DHA, and the selectivity of DHA was 64 and 92%, respectively. The basic sites promoted the formation of GLA, and the maximum selectivity to GLA (45%) was resulted from Au/MgAl-HTs. Therefore, the coexistence of Cu^+ sites and basic sites affect both the conversion and selectivity of Au in the GL oxidation to DHA. The effect depended on the ratio of Cu^+ sites to basic sites. Under Cu/Mg/Al molar ratio of 1:9:1 and optimum reaction conditions (60 °C, 6 h, and 0.088 g of 1 wt% Au/CuMgAl-HTs catalyst), the conversion of GL reached 53%, and the selectivity to DHA was up to 72%.

Funding This work was supported by projects funded by the Major Research Plan of National Natural Science Foundation of China (Program No. 91545130).

References

1. Ricapito NG, Ghobril C, Zhang H, Grinstaff MW, Putnam D (2016) Synthetic biomaterials from metabolically derived synthons. Chem Rev 116:2664–2704
2. Besson M, Gallezot P, Pinel C (2013) Conversion of biomass into chemicals over metal catalysts. Chem Rev 114:1827–1870
3. Villa A, Dimitratos N, Chan-Thaw CE, Hammond C, Prati L, Hutchings GJ (2015) Glycerol oxidation using gold-containing catalysts. Acc Chem Res 48:1403–1412
4. Jin X, Zhao M, Zeng C, Yan W, Song Z, Thapa PS, Subramaniam B, Chaudhari RV (2016) Oxidation of glycerol to dicarboxylic acids using cobalt catalysts. ACS Catal 6:4576–4583
5. Garcia AC, Kolb MJ, van Nieropy SC, Vos J, Birdja YY, Kwon Y, Tremiliosi-Filho G, Koper MTM (2016) Strong impact of platinum surface structure on primary and secondary alcohol oxidation during electro-oxidation of glycerol. ACS Catal 6:4491–4500
6. Hu W, Knight D, Lowry B, Varma A (2010) Selective oxidation of glycerol to dihydroxyacetone over Pt–Bi/C catalyst: optimization of catalyst and reaction conditions. Ind Eng Chem Res 49:10876–10882
7. Lari GM, Mondelli C, Pérez-Ramírez J (2015) Gas-phase oxidation of glycerol to dihydroxyacetone over tailored iron zeolites. ACS Catal 5:1453–1461
8. Zhou CH, Beltramini JN, Fana Y, Lu GQ (2008) Chemoselective catalytic conversion of glycerol as a biorenewable source to valuable commodity chemicals. Chem Soc Rev 37:527–549
9. Dimitratos N, Lopez-Sanchez JA, Anthonykutty JM, Brett G, Carley AF, Knight DW, Hutchings GJ (2009) Oxidation of glycerol using gold-palladium alloy-supported nanocrystals. Phys Chem Chem Phys 11:4952–4961
10. Liu S, Sun K, Xu B (2014) Specific selectivity of Au-catalyzed oxidation of glycerol and other C3-polyols in water without the presence of a base. ACS Catal 4:2226–2230
11. Villa A, Campisi S, Mohammed KMH (2015) Tailoring the selectivity of glycerol oxidation by tuning the acid–base properties of Au catalysts. Catal Sci Technol 5(2):1126–1132
12. Carrettin S, McMorn P, Johnston P, Griffin K, Hutchings GJ (2002) Selective oxidation of glycerol to glyceric acid using a gold catalyst in aqueous sodium hydroxide. Chem Commun 7:696–697
13. Carrettin S, McMorn P, Johnston P, Griffin K, Kiely CJ, Hutchings GJ (2003) Oxidation of glycerol using supported Pt, Pd and Au catalysts. Phys Chem Chem Phys 5:1329–1336
14. Xu C, Sun J, Zhao B, Liu Q (2010) On the study of KF/Zn(Al)O catalyst for biodiesel production from vegetable oil. Appl Catal B 99: 111–117
15. Wang H, Liu D, Xu C (2016) Directed synthesis of well dispersed and highly active AuCu and AuNi nanoparticle catalysts. Catal Sci Technol 6:7137–7150
16. Sing KSW, Everett DH, Haul RAW, Moscou L, Pierotti RA, Rouquerol J, Siemieniewska T (1985) Reporting physisorption data for gas/solid systems with special reference to the determination of surface area and porosity. Pure Appl Chem 57:603–619
17. Xu J, Yue H, Liu S, Wang H, Du Y, Xu C, Dong W, Liu C (2016) Cu-Ag/hydrotalcite catalysts for dehydrogenative cross-coupling of primary and secondary benzylic alcohols. RSC Adv 6:24164–24174
18. Deutsch KL, Shanks BH (2012) Active species of copper chromite catalyst in C-O hydrogenolysis of 5-methylfurfuryl alcohol. J Catal 285:235–241
19. Dai W, Sun Q, Deng J, Wu D, Sun Y (2001) XPS studies of Cu/ZnO/Al_2O_3 ultra-fine catalysts derived by a novel gel oxalate co-precipitation for methanol synthesis by CO_2+H_2. Appl Surf Sci 177:172–179
20. Santoro F, Psaro R, Ravasio N, Zaccheria F (2014) N-alkylation of amines through hydrogen borrowing over a heterogeneous Cu catalyst. RSC Adv 4:2596–2600
21. Luggren PJ, Apesteguıa CR, Cosimo JI (2016) Conversion of biomass-derived 2-hexanol to liquid transportation fuels: study of the reaction mechanism on Cu-Mg-Al mixed oxides. Top Catal 59: 196–206
22. Porta F, Prati L (2004) Selective oxidation of glycerol to sodium glycerate with gold-on-carbon catalyst: an insight into reaction selectivity. J Catal 224:397–403